

# Extremely Fe-rich metamorphic sekaninaite in a sillimanite-grade schist clast from the Middle Jurassic conglomerate, Hida Mountains, Japan

Tatsuki TSUJIMORI<sup>1,\*</sup>

Accepted on October 31, 2003

**Abstract** Extremely Fe-rich metamorphic sekaninaite (Fe<sup>2+</sup>-dominant analogue of cordierite) with 0.16–0.21 Mg/(Mg+Fe<sup>2+</sup>) ratio was found in a cobble of garnet-sillimanite schist from Middle Jurassic conglomerate (Tetri Group) in the Hida Mountains, Japan. Sekaninaite occurs as reaction corona replacing relict porphyroblastic almandine-rich garnet; it contains 0.17–0.35 wt.% Na<sub>2</sub>O. Microtextural relationship defines the primary stage ( $M_1$ : Grt + Bt + Sil) and the sekaninaite-forming stage ( $M_2$ : Sek + Bt + Sil). The sekaninaite-bearing phase equilibria constrains a qualitative metamorphic condition of  $T = 610$ – $790^\circ\text{C}$  and  $P = 60$ – $320$  MPa for the  $M_2$ , and suggests a decompressional cooling path from the  $M_1$  ( $P = c. 330$  MPa at nominal  $T = 740^\circ\text{C}$ ). Fe-rich sekaninaite composition may reflect unusually low Mg/(Mg+Fe<sup>2+</sup>) ratio (0.14) of bulk-rock composition.

**Keywords:** sekaninaite, Fe-cordierite, metapelite, sillimanite grade, Tetri Group, Hida Mountains

## INTRODUCTION

The cordierite group mineral is common in low-pressure (LP) granulite and migmatite terranes. Most metamorphic cordierite group minerals are Mg-rich with more than 0.5  $X_{\text{Mg}}$  [=Mg/(Mg+Fe<sup>2+</sup>) ratio] (e.g., Leake, 1960; Bhattacharya et al., 1988). On the other hand, Fe<sup>2+</sup>-rich cordierite, sekaninaite, has very restricted occurrences as a primary phase in felsic igneous rock and migmatite (e.g. Stanke and Miskovsky, 1964; Cerny et al., 1997; Hiroi et al. 2001; Rapela et al. 2002). Although sekaninaite-forming reaction in the system KFLASH (K<sub>2</sub>O-FeO-Al<sub>2</sub>O<sub>3</sub>-SiO<sub>2</sub>-H<sub>2</sub>O) has been experimentally determined or thermodynamically calculated (e.g., Richardson, 1968; Mukhopadhyay and Holdaway 1994), the results indicate that this phase is stable as a subsolidus phase in high- $T$  metamorphic rocks. However, metamorphic sekaninaite has scarcely been described in natural parageneses (e.g., Spear and Chaney, 1989).

Extremely Fe-rich metamorphic sekaninaite (0.16–0.21  $X_{\text{Mg}}$ ) was recently found in a sillimanite-grade metapelite clast from Middle Jurassic conglomerate unit at Hida Mountains, Japan. Parageneses and compositions of sekaninaite and its associated minerals from this high-grade metapelite are investigated. Such unusual occurrence was interpreted in terms of bulk composition and  $P$ - $T$  conditions. Mineral abbreviations are after Kretz (1983) except for sekaninaite (Sek) throughout this paper.

well-rounded cobble (10 × 8 cm) in a Middle Jurassic conglomerate bed of the Tetori Group at Kuzuryu area, central Japan (Fig. 1). The Tetori Group unconformably overlies Hida Triassic Barrovian-type gneiss-schist terrane in the Hida Mountains. Clasts of the conglomerate bed consist mainly of quartzite, granite, marble, metapelite and sandstones (e.g., Yamada et al., 1989); Tsujimori (1995) described a staurolite-sillimanite schist cobble possibly derived from the Hida terrane.

The sample is a medium-grained and well-foliated metapelite; no anatextic texture such as leucosome was observed. It consists mainly of fibrous sillimanite, quartz, garnet, and sekaninaite with minor amount of biotite, plagioclase (An<sub>6.8</sub>) and ilmenite, and trace K-feldspar, monazite, and apatite. Sekaninaite occurs as reaction coronas around relict garnet porphyroblasts (Fig. 2a, 2b and 2c) and a rare matrix phase. The corona is composed mainly of mosaic aggregates of sekaninaite with tiny inclusions of biotite, quartz, ilmenite, apatite and rare monazite. The original size of garnet porphyroblast may reach up to 7 mm in diameter, judged from the shape of reaction corona. Relict garnet contains inclusions of tiny ilmenite, quartz and apatite. Microtextural relationship indicates two stages of metamorphic recrystallization: the  $M_1$  stage assemblage includes garnet porphyroblast setting in a foliated matrix of Sil + Bt ( $M_1$ ) + Pl + Qtz and the  $M_2$  assemblage consists of Sek + Bt ( $M_2$ ) + Qtz. Sekaninaite was formed by the breakdown of garnet and is the most characteristic phase for the  $M_2$  event. Secondary chlorite and sericite locally replace sekaninaite.

## SAMPLE DESCRIPTION AND PETROGRAPHY

Sekaninaite-bearing schist sample (TD-KZ4/6) was collected as a

<sup>1</sup> Research Institute of Natural Sciences, Okayama University of Science, Okayama 700-0005, Japan

\* Corresponding author. E-mail; tatsukix@rins.ous.ac.jp

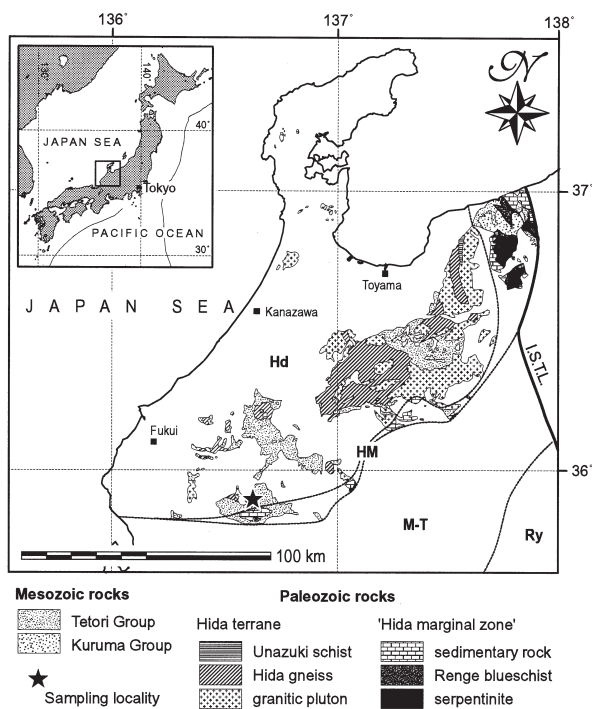


Fig. 1. Distribution map of pre-Cretaceous rocks in the Hida Mountains, Japan (after Tsujimori, 2002) and the locality of the Kuzuryu area. Hd = Hida terrane; HM = Hida marginal zone; M-T = Mino-Tamba accretionary complex; Ry = Ryoke LP metamorphic belt; I.S.T.L. = Itoigawa-Shizuoka Tectonic Line.

### WULK-ROCK CHEMISTRY

Bulk-rock composition of the sekaninaite-bearing sample was analyzed by a Rigaku System 3270 X-ray fluorescence spectrometer with Rh tube at Kanazawa University; the operating conditions were 50 kV accelerating voltage and 20 mA beam current. The result is given in Table 1. It is characterized by high in  $\text{Al}_2\text{O}_3$  (26.0 wt.%),  $\text{SiO}_2$  (57.2 wt.%) and total iron oxide as FeO (12.4 wt.%), but low in  $\text{K}_2\text{O}$  (0.7 wt.%),  $\text{MgO}$  (1.2 wt.%),  $\text{CaO}$  (1.2 wt.%) and  $\text{Na}_2\text{O}$  (2.4 wt.%), with 27 mol% normative corundum, 38 mol% quartz and 21 mol% normative albite; the  $\text{Mg}/(\text{Mg}+\text{Fe})$  and  $\text{Al}_2\text{O}_3/(\text{CaO} + \text{Na}_2\text{O} + \text{K}_2\text{O})$  molar ratios are 0.14 and 3.55, respectively. This highly peraluminous and iron-rich features suggest that the protolith has originated as bauxitic supracrustal sediment.

### MINERAL CHEMISTRY

Electron microprobe analysis and X-ray element mapping were carried out with a JEOL JXA-8800R at Kanazawa University. The quantitative analyses of rock-forming minerals were performed with 15 kV accelerating voltage, 12 nA beam current and 3–5  $\mu\text{m}$  beam size. Natural and synthetic silicates and oxides were used as standards. The ZAF method (oxide basis) was employed for matrix corrections. Representative analyses of sekaninaite and other minerals are listed in Table 2; compositions of these minerals and rock are

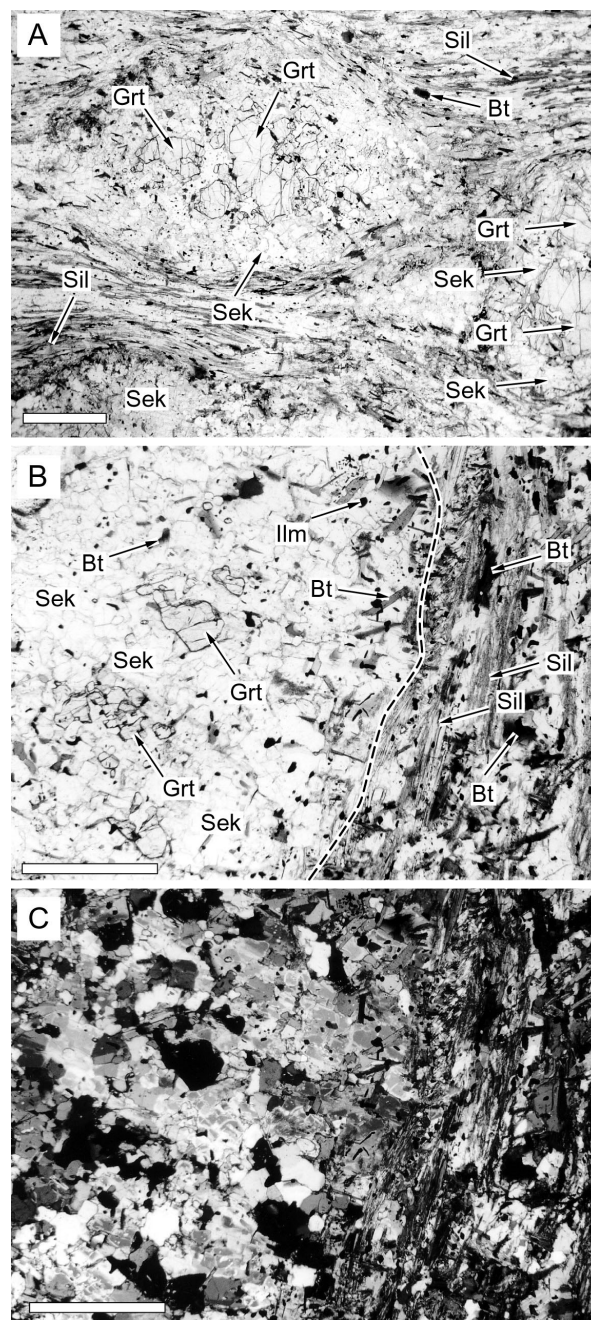


Fig. 2. Photomicrograph showing microtexture of sekaninaite in garnet-sillimanite schist. (A) Plane-polarizer view showing sekaninaite replacing porphyroblastic garnet; preferred orientation of fibrous sillimanite defines a foliation. Scale bar represents 1 mm. (B) Enlarged image of coronitic sekaninaite; sekaninaite contains biotite and quartz. Scale bar represents 0.5 mm. (C) Cross-polarizer view of (B).

plotted in an AFM diagram of Figure 3.

**Sekaninaite.** Sekaninaite contains essentially 16.9–18.2 wt% FeO as total Fe, 30.9–32.0 wt%  $\text{Al}_2\text{O}_3$ , 46.2–47.3 wt%  $\text{SiO}_2$  with less than 2.6 wt%  $\text{MgO}$  and 0.35 wt%  $\text{Na}_2\text{O}$  (0.04–0.07 Na p.f.u. for O=18); the analysed sekaninaite shows a negative correlation of Si against Na + Al, indicating a substitutions Si in tetrahedral site  $\leftrightarrow$  Na in channel site plus Al in tetrahedral site (Wolfsdorff and Schreyer 1992). The  $X_{\text{Mg}}$  of sekaninaite varies from 0.16 to 0.21; no systematic chem-

ical difference is observed in spite of their occurrences. Anhydrous total of analyzed oxides add to only 98.0-99.2 wt.% suggesting appreciable content of volatile molecules.

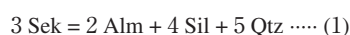
**Garnet (relict).** Relict garnet is enriched in almandine component with minor pyrope, spessartine and grossular components ( $\text{Prp}_{2-4}\text{Alm}_{92-93}\text{Sps}_{2-5}\text{Grs}_{<1}$ ). The  $X_{\text{Mg}}$  varies from 0.02 to 0.03. Core of relict garnet has slightly high Mn content.

**Biotite.** The matrix  $M_1$  biotite contains 1.1-1.4 wt.%  $\text{TiO}_2$  whereas  $M_2$  biotite inclusions in coronitic sekaninaite contains 2.4-3.2 wt.%  $\text{TiO}_2$ . The  $X_{\text{Mg}}$  of the  $M_1$  biotite and  $M_2$  biotite are 0.15-0.16 and 0.10-0.13, respectively.

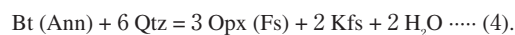
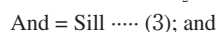
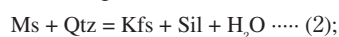
**Other minerals.** Sillimanite contains 0.1-0.2 wt.%  $\text{Fe}_2\text{O}_3$ . Ilmenite in coronitic sekaninaite contains up to 2.0 wt.% MnO.

### P-T CONDITION FOR THE SEKANINAITE-FORMATION

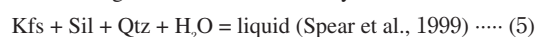
In the studied sample, the coronitic replacement of sekaninaite after porphyroblastic garnet can be expressed by one reaction in the KFMASH system such as



The end-member reaction in Mg-free system has been experimentally determined and thermodynamically calculated (e.g. Richardson, 1968; Mukhopadhyay and Holdaway, 1994), and constrains a maximum  $P < 200$  MPa at  $T = 700$ -750 °C (Mukhopadhyay and Holdaway 1987). In the KFMASH system with excess Qtz + Kfs +  $\text{H}_2\text{O}$ , the  $P$ - $T$  limit of the  $M_2$  Sek + Bt + Sil assemblage is defined by the following reactions together with reaction (1) (Fig. 5):



Moreover, no textural evidence of anatexis suggests that the vapor-saturated melting reaction in the KASH system



constrains the high- $T$  limit of the  $M_2$  assemblage. The  $P$ - $T$  condition for the  $M_2$  was calculated using the software BAYES (Chatterjee et al., 1998) with activities of minerals 0.66 for sekaninaite, 0.75 for garnet and 0.18 for biotite (annite) and 1.0 for the other phases to be  $T = 610$ -790 °C and  $P = 60$ -320 MPa (Fig. 5). The activity models for such estimates are based on Holland and Powell (1998). The moderate Na contents (up to 0.06 p.f.u.) of sekaninaite further support the estimated  $T$  condition (Mireald, 1986; Kalt et al., 1998).

On the other hand, the  $P$ - $T$  condition of the  $M_1$  assemblage may be constrained by the GASP geobarometer reaction,  $2 \text{ Sill} + \text{Grs} + \text{Qtz} = 3 \text{ An}$ . it gives an approximate  $P = \text{c. } 330$  MPa at nominal  $T = 740$  °C. This suggests that the metamorphic evolution from  $M_1$  to  $M_2$  is characterized by a decompressional cooling.

### COMPARISON WITH THE OTHER METAMORPHIC SEKANINAITE

Few metamorphic sekaninaites with higher  $X_{\text{Mg}}$  have been docu-

Table 1. Bulk-rock composition of sekaninaite-bearing schist.

Sample	TD-KZ4/6
$\text{SiO}_2$	52.46
$\text{TiO}_2$	1.62
$\text{Al}_2\text{O}_3$	25.97
$\text{FeO}^*$	12.35
MnO	0.20
MgO	1.16
CaO	1.18
$\text{Na}_2\text{O}$	2.14
$\text{K}_2\text{O}$	1.52
$\text{P}_2\text{O}_5$	0.04
Total	98.64
FeO* = total Fe as FeO.	

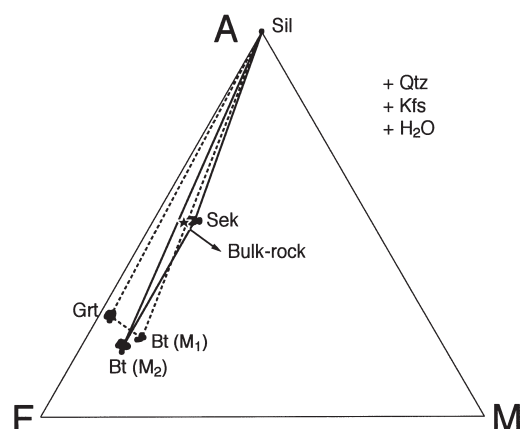


Fig. 3. AFM diagram projected from K-feldspar showing analyzed mineral compositions and a bulk-rock composition.

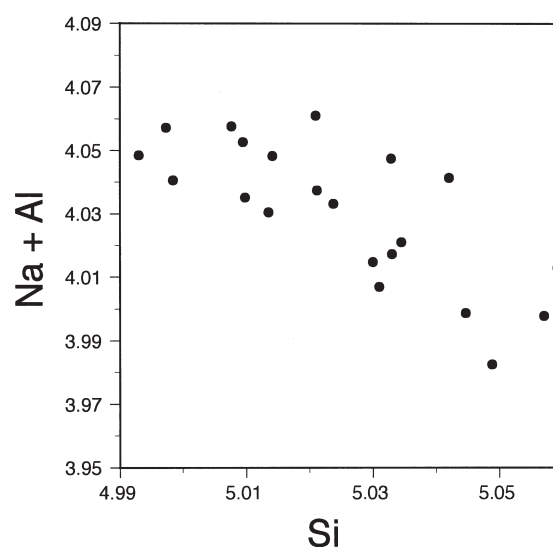


Fig. 4. Si versus (Na + Al) diagram showing the  $\text{Si} \rightleftharpoons \text{Na} + \text{Al}$  substitution of analyzed sekaninaite. The amounts of Si, Na and Al are calculated based on structural formulae units.



Table 2. Representative electron-microprobe analyses of sekaninaite, garnet, biotite, and plagioclase.

	Sekaninaite			Garnet		Biotite		Plagioclase	
	average (N=21)					M <sub>1</sub>	M <sub>2</sub>		
SiO <sub>2</sub>	46.69	46.96	46.84	37.15	36.74	33.57	33.78	65.51	66.27
TiO <sub>2</sub>	0.00	0.05	0.02	0.06	0.03	1.22	2.91	0.01	0.04
Al <sub>2</sub> O <sub>3</sub>	31.49	31.65	31.49	20.14	20.95	21.61	20.15	20.89	20.80
Cr <sub>2</sub> O <sub>3</sub>	0.00	0.00	0.00	0.00	0.00	0.00	0.05	0.06	0.00
FeO*	17.75	17.75	17.55	41.06	40.43	28.04	27.87	1.96	0.26
MnO	0.21	0.19	0.20	1.05	1.62	0.06	0.00	0.00	0.05
MgO	2.02	2.30	2.22	0.97	0.60	2.70	1.95	0.19	0.00
CaO	0.07	0.00	0.03	0.22	0.23	0.00	0.00	1.52	1.73
Na <sub>2</sub> O	0.22	0.24	0.24	0.03	0.00	0.18	0.20	10.42	10.86
K <sub>2</sub> O	0.00	0.00	0.00	0.00	0.00	9.25	9.31	0.13	0.05
Total	98.46	99.13	98.59	100.67	100.61	96.62	96.22	100.70	100.06
O <sub>2</sub>	18	18	18	12	12	22	22	8	8
Si	5.021	5.014	5.025	3.035	3.002	5.246	5.310	2.874	2.911
Ti	0.000	0.004	0.001	0.003	0.002	0.144	0.344	0.000	0.001
Al	3.991	3.982	3.981	1.938	2.017	3.980	3.732	1.080	1.077
Cr	0.000	0.000	0.000	0.000	0.000	0.000	0.006	0.002	0.000
Fe <sup>3+</sup>								0.065	0.009
Fe <sup>2+</sup>	1.596	1.585	1.574	2.805	2.762	3.665	3.664		
Mn	0.019	0.017	0.019	0.073	0.112	0.008	0.000	0.000	0.002
Mg	0.324	0.366	0.354	0.118	0.073	0.629	0.457	0.012	0.000
Ca	0.008	0.000	0.004	0.019	0.020	0.000	0.000	0.072	0.081
Na	0.046	0.049	0.050	0.004	0.001	0.054	0.059	0.886	0.925
K	0.000	0.000	0.000	0.000	0.000	1.844	1.866	0.007	0.003
Total	11.006	11.016	11.008	7.995	7.988	15.569	15.440	4.999	5.009
X <sub>Mg</sub>	0.17	0.19	0.18	0.03	0.01	0.15	0.11		

FeO\* = total Fe as FeO. X<sub>Mg</sub> = Mg/(Mg+Fe<sup>2+</sup>)

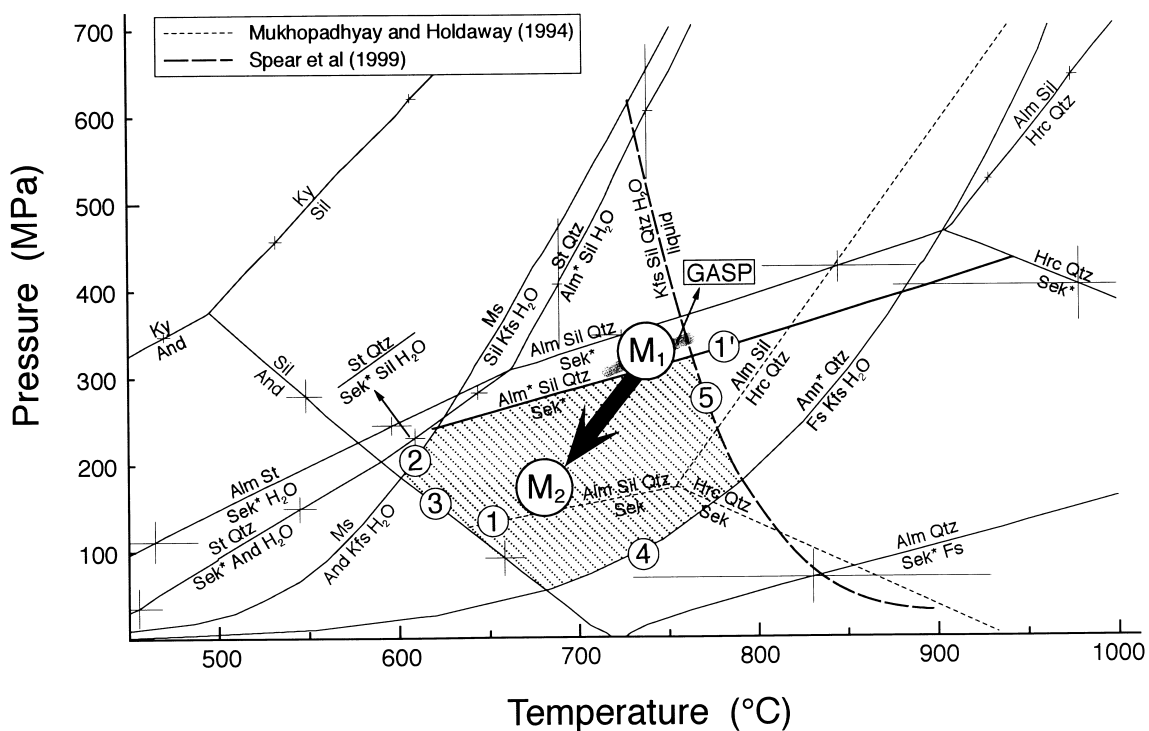


Fig. 5. *P-T* diagram showing selected phase relationships and a qualitative *P-T* estimations. All reactions of solid lines are calculated by the software BAYES (Chatterjee et al., 1998); crossed bars represent 1  $\sigma$  error of the calculation. Mineral abbreviations with '\*' represent minerals with fixed activities as < 1.0 (see text). The melting reaction (5) is after Spear et al. (1999). Dashed lines involving reaction (1) are after Mukhopadhyay and Holdaway (1994). The reactions curves of (1') represents an isopleths of the reactions (1).

mented. For examples, those with  $X_{\text{Mg}} > 0.28$  in metapelite of a contact aureole from the Island of Kos (Greece) coexist with biotite, andalusite, garnet, hercynite and rare sillimanite (Kalt et al., 1998); most of them were formed at the andalusite-stability field. Relict chloritoid is preserved in some sekaninaites of this locality according to a chloritoid-consuming reaction:  $\text{Cld} = \text{Crd} + \text{Hrc} + \text{H}_2\text{O}$ ; the  $P$ - $T$  condition was estimated to be  $P < 400$  MPa at  $T = 510$ - $750$  °C. Metamorphic sekaninaites with  $X_{\text{Mg}} > 0.40$  in pelitic granulite from the Nain complex, Labrador have been described by Berg (1977). They coexist with garnet and sillimanite or orthopyroxene;  $P = 370$ - $660$  MPa at  $T < 915$  °C was estimated. The characteristics in these two cases are that the constituent minerals coexisting with sekaninaite are characterized by very low  $X_{\text{Mg}}$ . This indicates that the  $X_{\text{Mg}}$  of sekaninaite is not only attributed to Fe-Mg partitioning during continuous reaction but also strongly depends on Fe-rich bulk-rock composition.

The investigated sekaninaite from Japan is characterized by extremely low  $X_{\text{Mg}}$  (0.16-0.21). This may reflect unusually Fe-rich and very low  $X_{\text{Mg}}$  (0.14) for bulk rock composition. Although metamorphic sekaninaite is less common in the natural parageneses, it may appear stably at LP condition but in wide  $T$  range from the andalusite field to high above a granitic water-saturated solidus in the sillimanite field. However, the sekaninaite stability overlaps in the anatexitic conditions of LP metapelites. At  $P < c. 400$  MPa of the sillimanite field, a continuous dehydration melting reaction,  $\text{Crd} (\text{Sek}) + \text{Bt} = \text{Grt} + \text{Sil} + \text{liquid}$ , may occur in the KFMASH ( $M = \text{MgO}$ ) or NKFASH ( $N = \text{Na}_2\text{O}$ ) systems (e.g. Brown, 1998; Spear et al., 1999). As the melting reaction has a negative slope, sekaninaite-consuming dehydration melting will occur with prograde evolution of LP pelitic rocks; the reaction shifts to lower  $T$  and  $P$  sides with decreasing bulk rock  $X_{\text{Mg}}$ . In the prograde LP metamorphic terranes and aureole, the sekaninaite-consuming melting may cause the rare occurrence of natural-metamorphic sekaninaite, even if the bulk-rock compositions to form sekaninaite are satisfied.

#### ACKNOWLEDGEMENT

This research was supported financially in part by JSPS Research Fellowship for Young Scientists, and Grant-in-Aid for JSPS Fellows. The author thanks to H. Shukuno for helping XRF analysis. This manuscript has been critically reviewed by J.G. Liou.

#### REFERENCES

- Berg, J.H., 1977. Regional geobarometry in the contact aureoles of the anorthitic Nain Complex, Labrador. *Journal of Petrology*, **18**, 399-430.
- Bhattacharya, A., Mazumdar, A.C. and Sen, S.K., 1988. Fe-Mg mixing in cordierite: constraints from natural data and implications for cordierite-garnet geothermometry in granulites. *American Mineralogist*, **73**, 338-344.
- Brown, M., 1998. Unpairing metamorphic belt: P-T paths and a tectonic model for the Ryoke Belt, southwestern Japan. *Journal of Metamorphic Geology*, **16**, 3-22.
- Cerny, P., Chapman, P., Schreyer, W., Ottolini, L., Bottazzi, P., and McCammon, C.A., 1997. Lithium in sekaninaite from the type locality, Dolni Zbory, Czech Republic. *Canadian Mineralogist*, **35**, 167-173.
- Chatterjee, N.D., Krüger R., Haller G. and Olbricht W., 1998. The Bayesian approach to an internally consistent thermodynamic database: theory, database, and generation of phase diagrams. *Contributions to Mineralogy and Petrology*, **133**, 149-168.
- Holland, T.J.B. and Powell, R., 1998. An internally consistent thermodynamic data set for phases of petrological interest. *Journal of Metamorphic Geology*, **16**, 309-343.
- Kalt, A., Altherr, R. and Ludwig, T., 1998. Contact metamorphism in pelitic rocks on the Island of Kos (Greece, Eastern Aegean Sea): a test for the Na-in-cordierite thermometer. *Journal of Petrology*, **39**, 663-688.
- Kretz, R., 1983. Symbols for rock forming minerals. *American Mineralogist*, **68**, 277-279.
- Leak, B.K., 1960. Compilation of chemical analysis and physical constants of natural cordierite. *American Mineralogist*, **45**, 282-298.
- Mirwald, P.W., 1986. Ist cordierite ein geothermometer. *Fortschritte der Mineralogie*, **64**, 119.
- Mukhopadhyay, B. and Holdaway, M.J., 1994. Cordierite-garnet-sillimanite-quartz equilibrium: I. New experimental calibration in the system  $\text{FeO-Al}_2\text{O}_3\text{-SiO}_2\text{-H}_2\text{O}$  and certain P-T- $X_{\text{H}_2\text{O}}$  relations. *Contributions to Mineralogy and Petrology*, **116**, 462-472.
- Rapela, C.W., Baldo, E.G., Pankhurst, R.J. and Saavedra, J. (2002) Cordierite and leucogranite formation during emplacement of highly peraluminous magma: the El Pilon granite complex (Sierras Pampeanas Argentina). *Journal of Petrology*, **43**, 1003-1028.
- Richardson, S.W., 1968. Staurolite stability in a part of the system Fe-Al-Si-O-H. *Journal of Petrology*, **9**, 467-488.
- Spear, F.S. and Cheney, J.T., 1989. A petrogenetic grid for pelitic schists in the system  $\text{SiO}_2\text{-Al}_2\text{O}_3\text{-FeO-MgO-H}_2\text{O}$ . *Contributions to Mineralogy and Petrology*, **101**, 149-164.
- Spear, F.S., John, M.J. and Cheney, J.T., 1999. P-T paths from anatexitic pelites. *Contributions to Mineralogy and Petrology*, **134**, 17-32.
- Stanek, J. and Miskovsky, J., 1964. Zelezem bohaty cordierite z pegmatite od Dolnich Boru. *Caopis pro Mineralogii a Geologii*, **9**, 191-192.
- Thompson, J.B., 1957. The graphical analysis of mineral assemblages in pelitic schists. *American Mineralogist*, **42**, 842-858.
- Tsujimori, T., 1995. Staurolite-bearing sillimanite schist cobble from the Upper Jurassic Tetori Group in the Kuzuryu area, Hida Mountains, central Japan. *Journal of Geological Society of Japan*, **101**, 971-977.

- Tsujimori, T., 2002. Prograde and retrograde P-T paths of the late Paleozoic glaucophane eclogite from the Renge metamorphic belt, Hida Mountains, southwest Japan. *International Geology Review*, **44**, 797-818.
- Wolfsdorff, P. and Schreyer, W., 1992. Synthesis of sodium cordierites in the system  $\text{Na}_2\text{O}$ - $\text{MgO}$ - $\text{Al}_2\text{O}_3$ - $\text{SiO}_2$ . *Neues Jahrbuch für Mineralogie, Monatshefte*, **2**, 80-96.
- Yamada, K., Niwa, S. and Kamata, M., 1989. Lithostratigraphy of the Mesozoic Tetori Group in the upper reaches of the Kuzuryu River, central Japan. *Journal of Geological Society of Japan*, **95**, 391-403. (in Japanese with English abstract)